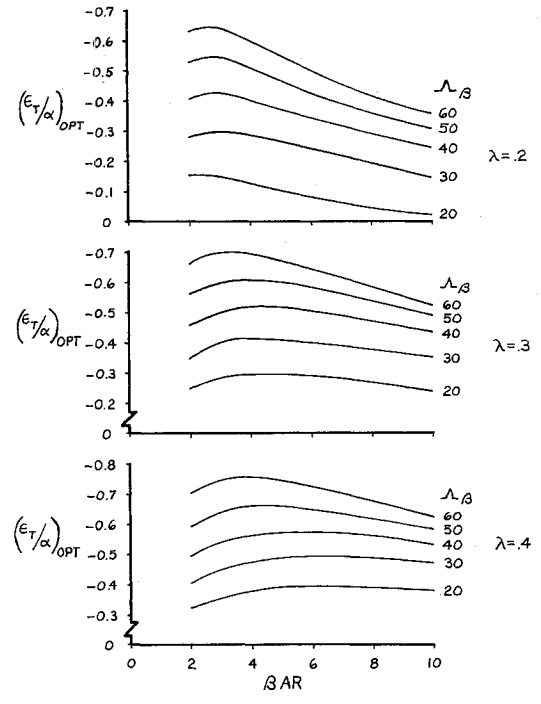

Fig. 5 Variation of optimum tip twist angle/angle-of-attack ratio with βAR.

attack ratio, which produces minimum induced drag for a particular wing, is defined as $(\epsilon_T/\alpha)_{OPT}$. Although this optimum cannot be defined with great precision (because of curve fits within the computer program used to calculate wing efficiency), the variation near the optimum is small, so that slight uncertainties will probably not be important for most practical applications. Figure 5 shows the variation of $(\epsilon_T/\alpha)_{OPT}$ with βAR for twisted, trapezoidal planform wings with taper ratios of 0.2, 0.3, and 0.4.

To design a wing of given planform to have a specified C_{L_D} and minimum induced drag, values of α_L, ϵ_T, and α_0 must be known. These can be determined as follows:

$$\alpha_L = C_{L_D}/C_{L_\alpha} \tag{3}$$

where C_{L_α} is obtained from Fig. 1;

$$\epsilon_T = \alpha_L(\epsilon_T/\alpha)_{OPT}/[1 + \alpha_{0_1}(\epsilon_T/\alpha)_{OPT}] \tag{4}$$

where α_{0_1} and $(\epsilon_T/\alpha)_{OPT}$ are obtained from Figs. 2 and 5, respectively; and

$$\alpha_0 = -(\alpha_{0_1})\epsilon_T \tag{5}$$

Thus all quantities needed for wing design are determined.

This note provides information that can be used to estimate rapidly the complete wing aerodynamic characteristics for any uncambered, flat-plate trapezoidal planform wing at subsonic Mach numbers including the linear-lofted twist needed to produce minimum induced drag for a specified lift coefficient. Data obtained from this procedure provide a good starting point for detailed consideration of more complex wing configurations.

References

[1] Martin, G. W., "Vortex collocation lifting surface theory for subsonic compressible potential flow," Lockheed-Georgia Co. Engineering Rept. ER-8814 (April 1967).

[2] Crigler, J. L., "Comparison of calculated and experimental distributions on thin wings at high subsonic and sonic speeds," NACA TN 3941 (January 1957).

[3] Jones, R. T. and Cohen, D., *High Speed Wing Theory* (Princeton University Press, Princeton, N. J., 1960), Princeton Aeronautical Paperbacks 6, Chap. 2, pp. 49–50.

[4] Sanders, K. L., "Subsonic induced drag," J. Aircraft **4**, 347–348 (1965).

Rolling Moment Due to Sideslip of Delta Wings

DAVID L. KOHLMAN*
University of Kansas, Lawrence, Kansas

Nomenclature

C_L	=	lift coefficient
C_l	=	rolling moment coefficient
β	=	angle of sideslip, rad
Λ	=	angle of sweepback, deg
Γ	=	dihedral angle, deg
C_{l_β}	=	$\partial C_l/\partial\beta\|_{\beta=0}$
$(\partial C_{l_\beta}/\partial C_L)_0$	=	$\partial C_{l_\beta}/\partial C_L\|_{C_L=0}$
$(\partial C_{l_\beta}/\partial C_L)_A$	=	contribution of aspect ratio to $(\partial C_{l_\beta}/\partial C_L)_0$
$(\partial C_{l_\beta}/\partial C_L)_\Lambda$	=	contribution of sweepback to $(\partial C_{l_\beta}/\partial C_L)_0$
A	=	aspect ratio

AN extensive literature survey has been conducted to correlate existing experimental data with various predictions of the rolling moment due to sideslip for delta wings.

For incompressible flow the rolling moment due to sideslip for an isolated wing is given by the equation

$$C_{l_\beta} = C_L\left[\left(\frac{\partial C_{l_\beta}}{\partial C_L}\right)_A + \left(\frac{\partial C_{l_\beta}}{\partial C_L}\right)_\Lambda\right] + \Gamma\left(\frac{\partial C_{l_\beta}}{\partial \Gamma}\right)$$

The portion of C_{l_β} which is a linear function of lift coefficient is composed of two terms. The first term, $(\partial C_{l_\beta}/\partial C_L)_A$, which is a function of aspect ratio and taper ratio, arises from two sources: the mutual induction of the leading and trailing wing panels, and the windward wing tip, which becomes effectively a leading edge with high negative pressures at the wing tip. The second term, $(\partial C_{l_\beta}/\partial C_L)_\Lambda$, is the contribution of sweepback to $(\partial C_{l_\beta}/\partial C_L)_0$. This contribution to rolling moment arises entirely from the difference in effective sweep angle and aspect ratio of the leading and trailing wing panels in sideslip.

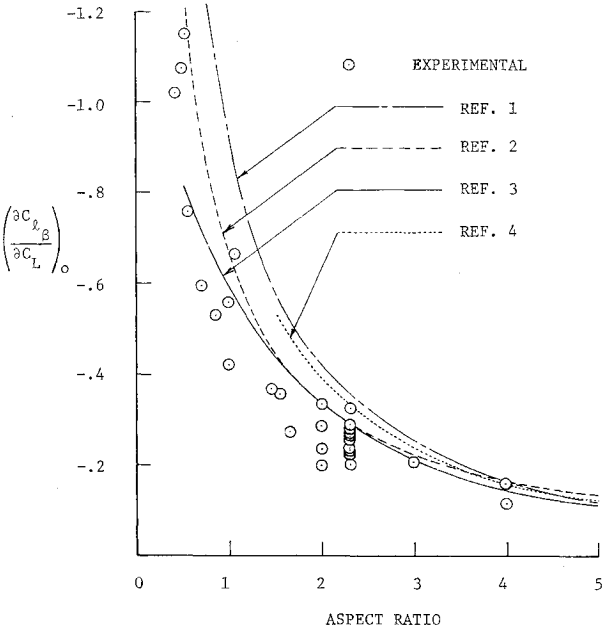

Fig. 1 Experimental and predicted values of $(\partial C_{l_\beta}/\partial C_L)_0$ for delta wings.

Received July 10, 1967; revision received August 10, 1967. Based on work performed for The Boeing Company under Boeing Purchase Order 6-253554-0966N. [3.01, 7.05]

* Associate Professor and Chairman, Department of Aerospace Engineering. Member AIAA.

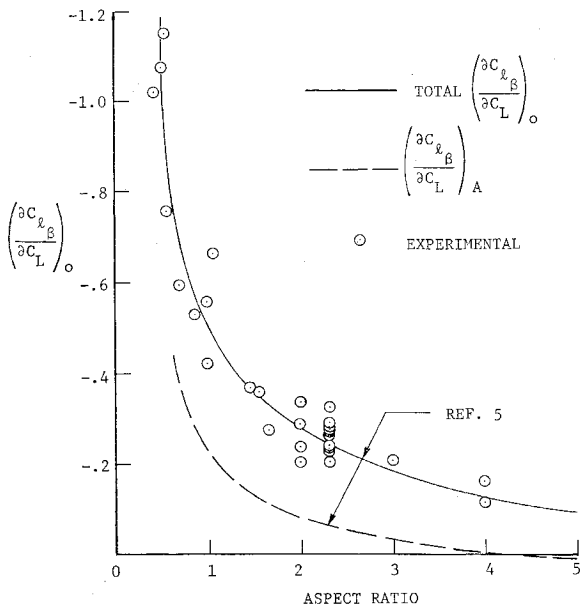

Fig. 2 Prediction for $(\partial C_{l\beta}/\partial C_L)_0$ for delta wings.

Figure 1 presents the data from a wide variety of experimental studies compared with the predictions resulting from the methods of four primary sources.[1-4] Clearly, all of the methods predict somewhat higher negative values of $(\partial C_{l\beta}/\partial C_L)_0$ than is justified by the average values of the experimental data points. Table 1 summarizes all of the experimental data.

A recent investigation by the author[5] includes the curve shown in Fig. 2 for predicting $(\partial C_{l\beta}/\partial C_L)_0$ for delta wings, which agrees quite well with the experimental data. The curve for $(\partial C_{l\beta}/\partial C_L)_A$ is included to show the relative effect of aspect ratio and sweepback.

One should note that $C_{l\beta}$ is a linear function of C_L only for low to medium lift coefficients for delta wings. The foregoing data apply only to the linear range. The derivative $(\partial C_{l\beta}/\partial C_L)_0$ was measured at $C_L = 0$.

There is presently no satisfactory empirical or theoretical method for predicting $C_{l\beta}$ in the nonlinear range. For delta wings, the nonlinear effects usually become significant at approximately $C_L = 0.5C_{L_{max}}$.

Table 1 Summary of delta wing experimental data

Reference	A	$-(\partial C_{L\beta}/\partial C_L)_0$ experimental
6	2.31	0.271
7	2.31	0.232
8	0.50	1.073
8	1.0	0.555
8	2.0	0.200
9	2.31	0.266
10	2.31	0.20
11	1.56	0.356
12	2.0	0.334
13	2.31	0.225
14	2.0	0.236
15	2.31	0.280
16	2.31	0.289
17	2.31	0.325
18	2.0	0.287
19	0.25	2.29
19	0.53	1.15
19	1.07	0.665
19	2.31	0.235
19	4.0	0.1145
19	6.93	0.573
20	3.0	0.206
21	0.42	1.02
21	0.56	0.757
21	0.71	0.595
21	0.85	0.528
21	1.00	0.420
21	1.46	0.367
22	2.31	0.286
22	4.0	0.16
23	1.66	0.272
24	2.31	0.254

References

[1] Polhamus, E. C. and Sleeman, W. C., Jr., "The rolling moment due to sideslip of swept wings at subsonic and transonic speeds," NASA TN D-209 (1960).

[2] Ribner, G., "The stability derivatives of low-aspect ratio triangular wings at subsonic and supersonic speeds," NACA TN 1423 (1947).

[3] Ellison, D. E., "USAF stability and control datcom," Douglas Aircraft Company Inc., Air Force Flight Dynamics Lab., Project 8219, Task 821902 revised (November 1965).

[4] Queijo, M. J., "Theoretical span load distributions and rolling moments for sideslipping wings of arbitrary plan form in incompressible flow," NACA Rept. 1269 (1955).

[5] Kohlman, D. L., *Handbook for Estimating $C_{l\beta}$ for Rigid and Elastic Airplanes at Subsonic and Supersonic Speeds* (University of Kansas Center for Research Inc., Lawrence, Kansas, March 1967).

[6] Goodman, A. and Thomas, D. F., Jr., "Effects of wing position and fuselage size on the low-speed static and rolling stability characteristics of a delta-wing model," NACA Rept. 1224 (1953).

[7] Fisher, L. R., "Experimental determination of effects of frequency and amplitude on the lateral stability derivatives for a delta, a swept, and an unswept wing oscillating in yaw," NACA Rept. 1357 (1956).

[8] Tosti, L. P., "Low-speed static stability and damping-in-roll characteristics of some swept and unswept low-aspect-ratio wings," NACA TN 1468 (October 1947).

[9] Riebe, J. M. and Moseley, W. C., Jr., "Low-speed static stability characteristics of a cambered-delta-wing model," NACA RM L55L21a (March 1956).

[10] Moseley, W. C., Jr., "Static stability characteristics of a cambered-delta-wing model at high subsonic speeds," NACA RM L56H13 (October 1956).

[11] Paulson, J. W., "Comparison of the static stability of a 68.7° delta-wing model with dihedral and a twisted and cambered wing model of the same plan form," NACA RM L55B11 (April 1955).

[12] Graham, D. and Koenig, D. G., "Tests in the Ames 40- by 80-foot wind tunnel of an airplane configuration with an aspect ratio 2 triangular wing and an all-movable horizontal tail—lateral characteristics," NACA RM A51L03 (February 1952).

[13] Johnson, J. L., Jr., "Low-speed measurements of static stability, damping in yaw, and damping in roll of a delta, a swept, and an unswept wing for angles of attack from 0° to 90°," NACA RM L56B01 (April 1956).

[14] Anderson, A. E., "An investigation at low speed of a large-scale triangular wing of aspect ratio two: I—characteristics of a wing having a double-wedge airfoil section with maximum thickness at 20 percent chord," NACA RM A7F06 (1947).

[15] Whittle, E. F., Jr. and Lovell, C. J., "Full scale investigation of an equilateral triangular wing having 10-percent-thick biconvex airfoil sections," NACA RM L8G05 (1948).

[16] Fletcher, H. S., "Low-speed experimental determination of the effect of leading-edge radius and profile thickness on static and oscillatory lateral stability derivatives for a delta wing with 60° of leading-edge sweep," NACA TN 4341 (July 1958).

[17] Lichtenstein, J. H. and Williams, J. L., "Effect of frequency of sideslipping motion on the lateral stability derivatives of a typical delta-wing airplane," NACA RM L57F07 (September 1957).

[18] Christensen, F. B., "An experimental investigation of four triangular-wing-body combinations in sideslip at Mach numbers 0.6, 0.9, 1.4, and 1.7," NACA RM A53L22 (March 1954).

[19] Letko, W., "Experimental determination at subsonic speeds of the oscillatory and static lateral stability derivatives of a series of delta wings with leading-edge sweep from 30° to 86.5°," NACA RM L57A30 (1957).

[20] Lange and Wacke, "Test report on three- and six-component measurements on a series of tapered wings of small aspect ratio," NACA TM 1176 (May 1948).

[21] Shanks, R. E., "Low-subsonic measurements of static and dynamic stability derivatives of six flat-plate wings having leading-edge sweep angles of 70° to 84°," NASA TN D-1822 (July 1963).

[22] Fournier, P. G., "Wind-tunnel investigation of the aerodynamic characteristics in pitch and sidelip at high subsonic speeds of a wing-fuselage combination having a triangular wing of aspect ratio 4," NACA RM L53G14A (1953).

[23] Unpublished data, Lockheed Supersonic Transport Configuration (1965).

[24] Llewellyn, C. P. and Wolhart, W. D., "Effect of Reynolds number on the lateral-stability derivatives at low speed of swept-back- and delta-wing-fuselage combinations oscillating in yaw," NASA TN D-398 (August 1960).

A Useful Method of Airfoil Stall Prediction

DAVID NORRIS REILLY*
Ewing Technical Design, Inc., Philadelphia, Pa.

Introduction

SYSTEMATIC investigations of airfoil stalling characteristics and their relation to the state of the boundary layer began with B. Melvill Jones in the mid 1930's. Jones[1,2] made what is probably the first generalization of stalling characteristics by classifying them into three types: a trailing-edge stall and two types of leading-edge stall. He postulated that stall could result from flow separation at the leading edge as well as the trailing edge, and observed the now well-known "bubble" or localized laminar flow separation.

Subsequent investigators explored the boundary layer and systematically varied the many parameters influencing the mechanism of transition and separation until the three principal types of stall, for which typical lift curves appear in Fig. 1, are now widely accepted: 1) trailing-edge stall, where there is a gradual loss of lift at high lift coefficient as the turbulent separation point moves forward from the trailing edge; 2) leading-edge stall, where there is an abrupt loss of lift, as the angle of attack for maximum lift is exceeded, with little or no rounding over of the lift curves; 3) thin-airfoil stall, where there is a gradual loss of lift at low lift coefficients as the turbulent reattachment point moves rearward.

Types of Stall

The top curve of Fig. 1 represents the lift variation on a typical rear-stalling airfoil. The Reynolds number is high enough that transition from a laminar to a turbulent boundary layer occurs before laminar separation can occur. Crabtree[3,4] has given, as an empirical condition for such a flow to exist, that the Reynolds number based upon the boundary-layer displacement thickness at separation be greater than 2700, $(R_{\delta^*})_s > 2700$. The first separation of the flow is then a turbulent one somewhere on the rear of the section.

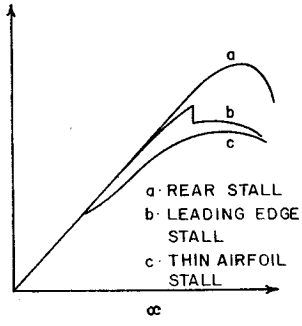

Fig. 1 Typical stalling curves.

The flows associated with leading-edge stall and thin-airfoil stall are characterized by the accompanying bubble, and typical lift curves appear as the center and lower curves, respectively, of Fig. 1. The laminar-separation bubble is characterized by a tangential separation from the airfoil surface with transition at maximum bubble height and the resulting turbulence spreading so that the flow reattaches. The velocity profiles in the separated layer up to transition are characteristic of those for laminar flow. Further downstream they are distorted by the transition process, and shortly after reattachment the profiles are typical of turbulent boundary layers. The static pressure within the bubble is nearly constant from the point of separation to the point of transition and then increases rapidly to the point of reattachment.

Owen and Klanfer[5] have classified bubbles as short if their length is of the order of 100 displacement thicknesses at separation, and long if their length is of the order of 10,000 displacement thicknesses at separation. They also determined a displacement thickness Reynolds number below which only long bubbles form and above which only short bubbles form. This value is between 400 and 500. Crabtree[6] more specifically has found the critical value to be between 400 and 450 when the calculation is based upon experimental pressure distributions and between 450 and 550 when based upon theoretical pressure distribution of potential flow.

The short bubble has a small effect on the over-all pressure distribution, and therefore lift and drag, as long as it reattaches. The long bubble, however, causes a collapse of the leading-edge suction with corresponding loss of lift and increase of drag.

Several criteria exist for the prediction of the laminar separation point. Curle and Skan suggest a form parameter $H = \delta^*/\Theta$, where Θ is the boundary-layer momentum thickness, exceeding 3.55.

Crabtree observed that there cannot be laminar reattachment at the rear of a bubble. There must be a considerable widening of the streamlines over the rear portion, and this necessitates a turbulent process. There are two principal mechanisms by which transition can occur in the boundary layer.

Tollmien-Schlichting waves are small, regular oscillations in the laminar boundary layer, not associated with freestream turbulence. These waves can amplify at their natural frequency of oscillation resulting in widespread turbulence. Schubauer and Skramstad[7] have determined a Reynolds number below which the boundary layer is stable for regular disturbances of any wave number.

Turbulent spots occur in a random manner near the upstream limit of the transition region. They spread laterally as wedges and are swept downstream at a velocity less than freestream. New spots are prevented from forming in the downstream region by the enhanced stability of the fluid between the growing turbulent wedges.

The turbulent spot process occurs only when $(R_{\delta^*})_s$ is greater than about 450 and takes place in a lesser length than that for amplification of waves. This has led to the general opinion that transition by the growth of turbulent spots occurs on short bubbles. On long bubbles $(R_{\delta^*})_s$ is usually less than 450, and they will not, in general, support the turbulent spot process. Transition is due to amplification of Tollmien-Schlichting waves.

The exact process and parameters involved in the breakdown of short bubbles are still a matter of some controversy, but it is generally agreed that there are two mechanisms for the process. Crabtree has postulated that bursting will occur

Received June 12, 1967. [3.01]
* Senior Aerodynamicist. Member AIAA.